Improved manometric setup for the accurate determination of supercritical carbon dioxide sorption

Patrick van Hemert,[1] Hans Bruining,[1,a)] E. Susanne J. Rudolph,[1] Karl-Heinz A. A. Wolf,[1] and Jos G. Maas[2]

[1]*Department of Geotechnology, Delft University of Technology, Delft 2628 CN, The Netherlands*
[2]*Shell International Exploration and Production, 2288 GS Rijswijk, The Netherlands*

An improved version of the manometric apparatus and its procedures for measuring excess sorption of supercritical carbon dioxide are presented in detail with a comprehensive error analysis. An improved manometric apparatus is necessary for accurate excess sorption measurements with supercritical carbon dioxide due to the difficulties associated with the high sensitivity of density for pressure and temperature changes. The accuracy of the apparatus is validated by a duplicate measurement and a comparison with literature data. Excess sorption and desorption of CO_2 on Filtrasorb 400 at 318.11 K up to 17 069 mole/m^3 (15.474 MPa) were selected for this validation. The measured excess sorption maximums are 7.79 ± 0.04 mole/kg at 2253 mole/m^3 for the first sorption isotherm and 7.91 ± 0.05 mole/kg at 2670 mole/m^3 for its subsequent desorption isotherm. The sorption and desorption peaks of the duplicate experiment are 7.92 ± 0.04 mole/kg at 2303 mole/m^3 and 8.10 ± 0.05 mole/kg at 2879 mole/m^3, respectively. Both data sets show desorption data being higher than the sorption data of the same data set. The maximum discrepancy between the desorption and sorption isotherms of one data set is 0.15 mole/kg. The discrepancy between the two excess sorption isotherms is 0.12 mole/kg or less. The *a priori* error of the excess sorption measurements is between 0.02 and 0.06 mole/kg. The error due to He contamination is between 0.01 and 0.05 mole/kg. The difference between the *a priori* uncertainty and the observed maximum discrepancies is considered to be acceptable. The sorption isotherms show identical qualitative behavior as data in the literature. The quantitative behavior is similar but the peak height and the linear decrease in excess sorption at high gas densities are 10% higher. A plot of the excess sorption versus the density can be used to obtain the sorbed phase density and the specific micropore volume. These sorbed phase densities are in excellent agreement with the data in the literature. Furthermore, the excess sorption data scaled to this specific micropore volume in this work and in the literature collapse on a single curve when plotted versus gas density. © *2009 American Institute of Physics.* [DOI: 10.1063/1.3063064]

I. INTRODUCTION

The amount of carbon dioxide (CO_2) that can be sorbed to coal plays an important role in the CO_2 storage in underground coalbeds. Accurate sorption experiments of near critical CO_2 on coal are required for the following applications: (1) acquisition of fundamental understanding of CO_2 sorption on coal, (2) determination of the economic feasibility of enhanced coalbed methane projects, and (3) determination of optimal operating conditions for CO_2 storage and methane (CH_4) production enhancement. A comprehensive overview on CO_2 storage in underground coal combined with the production of CH_4 is given by White *et al.*[1]

Experimental data of near supercritical CO_2 sorption on any type of material are scarce. A limited number of gravimetric,[2–13] manometric,[4,14–19] and volumetric[20,21] studies have been published. Additional measurements are thus important. Several researchers (e.g., Humayun and Tomasko[11] and Pini *et al.*[6]) have expressed their concern

with respect to the accuracy of supercritical CO_2 sorption determinations. The accuracy of the gravimetric method for supercritical CO_2 sorption has recently been discussed by Pini *et al.*[6] The focus of the present article is the accuracy of the manometric method.

The accuracy of the manometric method far below[22–27] and far above[28–31] the critical point has been discussed in the literature. However, no literature regarding the quantification of the accuracy of near critical manometric sorption measurements could be found. All the same, a number of references report experimental manometric sorption data of CO_2 on coal[4,14–16,18] and other materials[17,19] in the near critical region. Recent gravimetric sorption measurements of CO_2 on coal[3,5,7] show similar behavior, while recent manometric measurements vary considerably (e.g., in Ref. 4). It is the opinion of the author that these variations in the manometric experiments are artifacts. These artifacts are caused by small uncertainties in the pressure and temperature measurements and the presence of impurities. The proximity to the critical point magnifies these errors considerably.

In spite of the fact that the requirement of highly pure
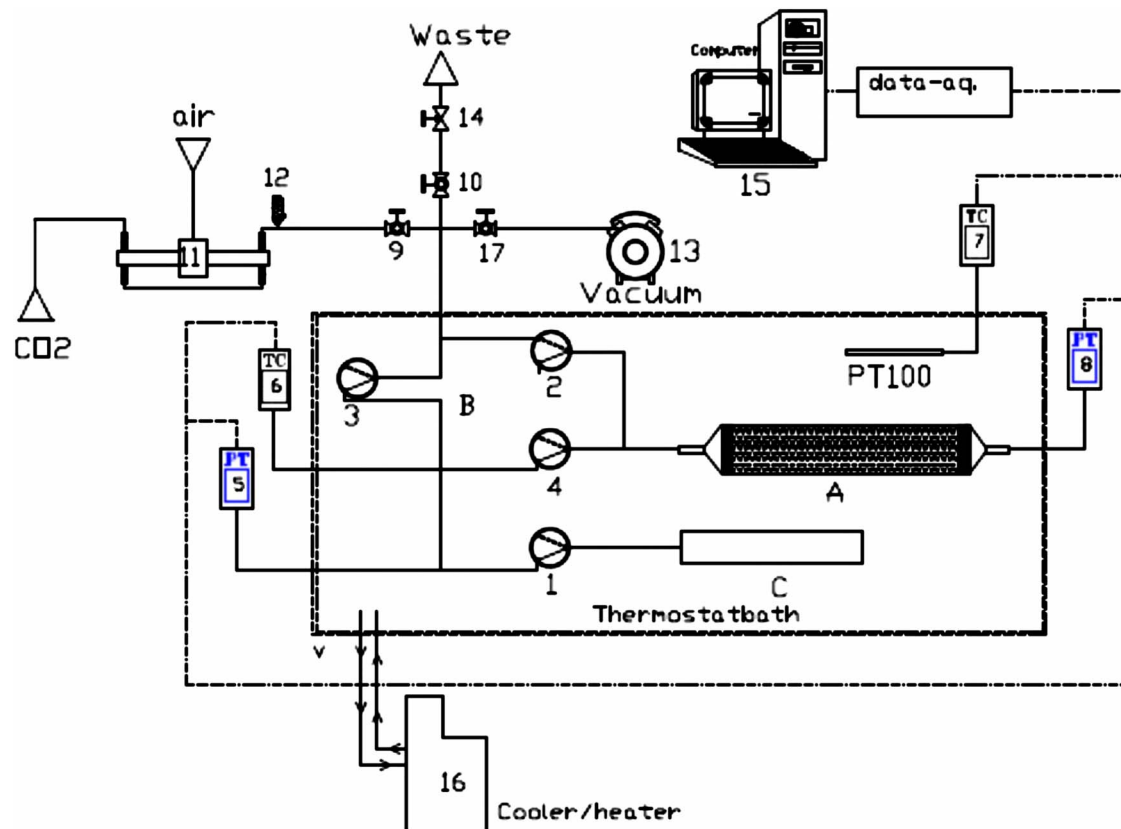
a)Electronic mail: j.bruining@tudelft.nl.

FIG. 1. (Color online) Technical drawing of the improved manometric apparatus.

CO_2 has been recognized, no article mentions the possible effects of contamination due to poor flushing and evacuation of the setup and its tubing. Using the Peng–Robinson equation of state (EOS) (Ref. 32) it can be shown that an impurity of 0.3 mol % of N_2 changes the density 2% at 10.000 MPa and 318.000 K. Other causes of artifacts are insufficient spatial and temporal temperature stability and inaccurate pressure and temperature measurements. For example, a 10 kPa and 0.10 K change at 10.000 MPa and 318.00 K changes the CO_2 density of 0.6% and 2.0%, respectively. The sensitivity of an excess sorption isotherm on density errors varies considerably. For example, an error of 2.0% in the density leads to an excess sorption error of 2%–70% for CO_2 excess sorption on F400 at 318.11 K, depending on which data point is influenced.

The accuracy of previous manometric experiments is impaired by the aforementioned errors. Therefore, we have developed a high accuracy manometric apparatus which reduced these errors with an order of magnitude. The main improvement of this apparatus is the better accuracy of the pressure and temperature sensors. Furthermore, the accuracy is estimated with a comprehensive *a priori* error analysis (see Appendix E). The apparatus, the sample treatment, and the experimental procedures are discussed in Sec. II. Duplicate sorption measurements of CO_2 on Filtrasorb 400 at 318.11 K are compared to each other and to literature data in Sec. III. Findings are summarized in Sec. III. Appendix A contains the derivation of the data interpretation equation, Appendix B contains demonstration of the small influence of He contamination on the excess sorption measurements,

Appendix C contains the leak-rate model, Appendix D contains demonstration of the negligibility of the influence of sorption on the leak-rate model, Appendix E contains an *a priori* uncertainty analysis, Appendix F contains the data processing procedure for the determination of the volume accessible to gas with a He experiment and Appendix G contains a concise explanation on regression of sorbed phase density ρ_{sorbed} and the specific micropore volume, $\bar{V}_{micropore}$, from excess sorption measurements.

II. EXPERIMENTAL METHODS

Manometric measurement of sorption is based on the principle of mass conservation. The excess sorption is defined as the difference between the total and the apparent amount of gas in the setup. The total amount is the sum of gas added minus gas extracted and leaked. The apparent amount of gas is determined by multiplication of the gas density with the volume accessible to gas. This volume is determined by He sorption experiments before and after the actual CO_2 experiment (see Appendix F).

A. Manometric apparatus

The manometric apparatus (Fig. 1 and Table I) consists of a sample cell (A) and reference cell (B: tubing-only cross in the middle of the figure). The reference cell B consists of tubing with a total volume of $3524 \pm 4 \times 10^{-9}$ m^3. The volume of the reference cell can be enlarged to $12\,152 \pm 9 \times 10^{-9}$ m^3 by opening valve 1 to include vessel C. The option of an enlargeable reference cell is new for this type of

TABLE I. Specification of setup components.

No.	Name, type	Manufacturer
1, 2, 3, 4	4 port 2-pos. valve, air actuated, N60/H	VICI ag international
5	Pressure transmitter, PTX600 0–250 bar	Druck Netherlands bv
6	Thermocouple, K-type	Thermocoax
7	Thermoelement PT100+F200 reader	Automated System Laboratories
8	Pressure transmitter, 9000 series	Paroscientific
9, 10, 17	Ball valve, SS-43S4	Swagelok NS&S
11	Gas booster air actuated, two stage	Haskel
12	Relief valve spring actuated, SS-RL3M4-S4	Swagelok NS&S
13	Vacuum pump, N820.3FT.40.18	KNF
14	Metering valve, SS-31-RS4	Swagelok NS&S
15	Data acquisition unit	Delft University Technology
16	Thermostat bath, Proline RP485	Lauda

setup. It allows better control of the amount of added and extracted gas. Two similar sample cells are used to minimize the downtime for a sample exchange. The volumes of these two sample cells are $7833 \pm 6 \times 10^{-8}$ and $7590 \pm 10 \times 10^{-8}$ m^3. The uncertainty in the empty sample cell volume does not affect the accuracy of the sorption data.

The stainless steel sample cell (A) was designed at Delft University of Technology. It holds a maximum of 6×10^{-5} m^3 of sorbent sample. The sample cell is sealed with Swagelok gaskets (SS-16-VCR-2GR) to minimize leakage. It contains filters of high porous sintered metal to minimize sample loss during the desorption run.

A Paroscientific pressure sensor (8) monitors the pressure continuously. Its precision and accuracy are reported by the manufacturer as 1 and 0.1 kPa in the temperature range of interest. The PT100 temperature sensor (7) monitors the temperature continuously. Its precision and accuracy are reported by the manufacturer as 1 and 20 mK. Less accurate pressure (5) and temperature sensors (6) are used to monitor pressure in the sample cell and temperature in the reference cell. However, the lower accuracy of these sensors precludes their use for excess sorption measurements. However, this does not affect the accuracy of the sorption data for which the higher accuracy sensors are used. Valves (1, 2, 3, and 4) have been selected based on their low leakage characteristics. However, they limit the experimental temperature to a maximum of 340 K. Furthermore, their internal diameter limits the evacuation of the setup to a minimum pressure between 15 and 25 kPa. The thermostatted bath has a volume of about 40×10^{-3} m^3. A temperature control device (16) keeps the temperature constant within 20 mK. The gas added to the setup is pressurized with a booster (11). The gas is extracted from the setup with an evacuation pump (13). All tubing is $1/8''$ Swagelok 316SS and only metal connections are used.

The PTX611 and the K-type thermocouple are connected to a Keithley KPCI-3108 data-acquisition and control card, which is connected to a personal computer with a 16 channel 16 bits single ended analog input. The Paroscientific pressure sensor and PT100 are connected to the PC through RS232 interfaces. The valves are controlled with a PC via the data-acquisition and control card. Control of the valves is on a time interval basis. The acquisition software is written in TESTPOINT V3.4. The acquisition software scans the measurements every second and records them every 10 s.

The Helium (He) has a purity of 99.996% and its critical properties are 5.1953 K, 227.46 kPa, and 17 399 mole/m^3. The CO_2 has a purity of 99.990% and its critical properties are 304.1282 K, 7.3773 MPa, and 10 624.9 mole/m^3. Gases are supplied by Linde Gas.

B. Sample selection and treatment

The experiments in this work are performed on Chemviron Filtrasorb 400, charge reference FE 05707A. This material, referred to as F400 in this article, is selected because it is a well-defined synthetic material with high sorption characteristics and its molecular structure and micropore size distribution are considered to be similar to coal. Furthermore, three other publications report the excess sorption of CO_2 at 318 K on other Filtrasorb 400s. This makes it the best represented sorbent in the literature for supercritical CO_2 sorption measurements. This good representation allows a comparison of the experimental data.

Prior to the sorption experiments the sample cell, already filled with F400, is evacuated for 24 h in an oven at a constant temperature of 473 K. To avoid air contamination the sample cell is filled with He above atmospheric pressure before its transfer from the oven to the setup. Sample weight is measured within 0.02 g during the transfer from the oven to the setup.

C. Experimental procedure

One experiment consists of the four following consecutive procedures: (1) He leak-rate determination, (2) determination of the volume accessible to gas by a He sorption experiment, (3) actual sorption experiment with CO_2, and (4) control measurement of the He sorption. The second He sorption experiment is performed to ensure that the volume accessible to gas has not changed during the experiment.

The He leak rate is determined at approximately 20 MPa and the experimental temperature for more than 24 h. The setup is evacuated at the experimental temperature for 24 h before the start of the sorption experiment. A sorption experi-

TABLE II. Specification of the experimental parameters. Mass density of F400 for He $\rho^{*,\text{F400,He}}$ is calculated with $M(V_{\text{empty}}^s - V^{s,\text{He}})^{-1}$.

	M ($10^{-5}\times$kg)	T (K)	$V^{s,\text{He}}$ ($10^{-7}\times$m^3)	$\rho^{*,\text{F400,He}}$ (kg/m^3)	k^{He} ($10^{-13}\times$m^3/s)	Duration CO_2 ($10^5\times$s)
Experiment 1	3495 ± 3	318.12 ± 0.02	592 ± 1	2080 ± 40	3.1	74.3
Experiment 2	3557 ± 1	318.11 ± 0.02	611 ± 1	2060 ± 40	2.1	4.3

ment consists of two parts: determination of the sorption isotherm followed by the desorption isotherm. For the sorption isotherm, gas is added stepwise to the evacuated sample cell until a pressure between 16 and 18 MPa is reached. For the desorption isotherm, gas is extracted sequentially from the sample cell until a pressure of 2–5 MPa is reached. Gas is added or removed after pressure and temperature have stabilized. Pressure stability is attained after 10^3 s for both CO_2 and He. However, time intervals longer than 10^3 s, i.e., 10^4 and 10^5 s, are used to ensure stability.

D. Data analysis

Measured properties are pressure and temperature; these are converted to density values, ρ in mole/m^3, using a highly accurate reference EOS.[33] The volume accessible to gas in the sample, $V^{s,\text{He}}$ in m^3, is determined from the He sorption experiments (see Appendix F). Sample mass, M in kg, is determined before the sample cell is built into the setup.

The excess amount of CO_2 sorbed is computed with Eq. (1) (derivation in Appendix A),

$$m_N^{\text{excess,CO}_2,\text{F400}} = \sum_{i=1}^{N} \frac{V_i^r}{M}(\rho_i^{f,\text{CO}_2} - \rho_i^{e,\text{CO}_2})$$
$$- \frac{\rho_N^{e,\text{CO}_2}V^{s,\text{He}} + n_N^{l,\text{CO}_2}}{M}, \qquad (1)$$

with

$$n_N^{l,\text{CO}_2} = \sum_{i=1}^{N} \rho_i^{e,\text{CO}_2}(V^{s,\text{He}} + V_i^r)[e^{t_i^e k^{\text{CO}_2}/(V^{s,\text{He}}+V_i^r)} - 1]$$
$$+ V^{s,\text{He}} \sum_{i=1}^{N-1} \rho_i^{e,\text{CO}_2}[1 - e^{-t_i^f k^{\text{CO}_2}/V^{s,\text{He}}}]. \qquad (2)$$

Here m_N^{excess} in mole/kg is the Nth determined excess sorption point. ρ_i^e is the gas density after stabilization of the reference and sample cell in step i. ρ_i^f is the stable gas density after gas addition to the reference cell for step i. n_N^l in mole is the cumulative gas leaked out of the sample cell at the Nth sorption determination (derivation in Appendix C). V_i^r is the volume of the reference cell used in step i. k in m^3/s is the leak-rate coefficient. t_i^e and t_i^f are the time taken for the equilibrium and filling phase, respectively.

The first term in Eq. (1) describes the summed difference between the number of moles in the reference cell for the filling and equilibrium phases. The second term describes the number of moles in the free phase in the sample cell. The first and second terms in Eq. (2) are the cumulative number of moles leaked during the equilibrium phases and filling phases, respectively.

III. RESULTS AND DISCUSSION

Table II shows the parameters for the two CO_2 sorption experiments. The determined mass density of F400 for the two experiments agrees within the experimental uncertainty. Figure 2 shows the two determined CO_2 excess sorption isotherms on F400 of this work and the literature data near 318 K on other F400s.[6,11,20] Experimental data of this work is shown in Table III.

The maxima of the excess sorption isotherms are 7.79 mole/kg at 2253 mole/m^3 and 7.92 mole/kg at 2303 mole/m^3. The maxima of the excess desorption isotherms are 7.91 mole/kg at 2670 mole/m^3 and 8.10 mole/kg at 2879 mole/m^3. The desorption isotherms of both experiments are higher than the corresponding sorption data. The maximum observed discrepancy between desorption and sorption data is 0.15 mole/kg. The discrepancy of the sorption data sets is less than 0.12 mole/kg. The *a priori* error estimate of the excess sorption measurements is 0.02–0.06 mole/kg. Appendix E discusses the various sources of uncertainty in detail. Figure 7 summarizes its results. The figure illustrates that the pressure and temperature measurements are sufficiently accurate at the chosen temperature of 318.11 K, i.e., density fluctuations are sufficiently small. The difference between the *a priori* uncertainty and the observed maximum discrepancies is acceptable. These differences can
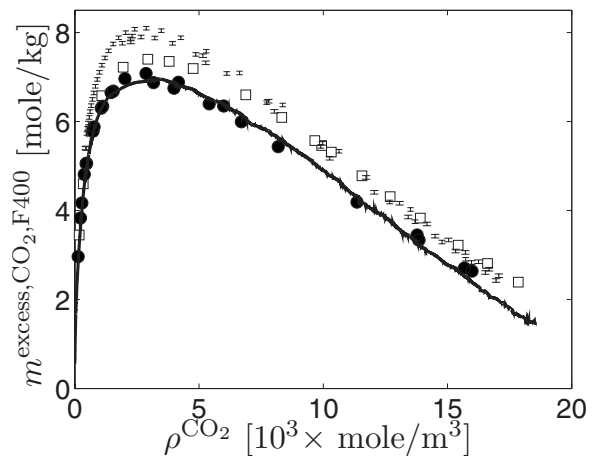

FIG. 2. CO_2 excess sorption data of this work (error bars) and literature data on F400 at 318 K. The data show typical excess sorption behavior. Excess sorption data increases sharply with gas density to a peak value of 7–8 mole/kg near 3.0×10^3 mole/m^3. The data decrease after the peak with a linear decrease for gas densities above 6×10^3 to 7×10^3 mole/m^3. The data from Humayun and Tomasko (Ref. 11) (line) and Fitzgerald *et al.* (Ref. 20) (filled circles) are lowest and in excellent agreement. The data of this work are in good internal agreement but 10% higher than the data of Tomasko and Gasem. The data from Pini *et al.* (Ref. 6) (open squares) are in between the data of this work and that of Tomasko and Gasem.

TABLE III. Excess sorption data of CO_2 on Chemviron Filtrasorb 400 at 318.11 K determined for this article. The number of data points in general is kept limited to keep cumulative errors in the desorption data at a minimum. The number of data points of the first data set is small to minimize the time required for the experiment.

Sorption 1		Desorp 2		Sorption 2		Desorp 2a		Desorp 2b	
ρ^{CO_2} (mole/m^3)	$m^{exc.}$ (mole/kg)	ρ^{CO_2} (mole/m^3)	$m^{exc.}$ (mole/kg)	ρ^{CO_2} (mole/m^3)	$m^{exc.}$ (mole/kg)	ρ^{CO_2} (mole/m^3)	$m^{exc.}$ (mole/kg)	ρ^{CO_2} (mole/m^3)	$m^{exc.}$ (mole/kg)
457	5.39	15 729	2.90	446	5.41	13 513	4.02	1215	7.43
2253	7.79	14 781	3.29	2303	7.92	10 636	5.33	1093	7.27
5270	7.32	13 697	3.75	5154	7.48	8368	6.37	991	7.10
8032	6.23	12 675	4.19	7791	6.46	6630	7.09	904	6.95
10 261	5.18	9900	5.44	9975	5.51	5293	7.58	830	6.79
12 054	4.41	7728	6.42	11 721	4.74	4269	7.88	766	6.64
13 419	3.86	6120	7.08	13 073	4.16	3483	8.04	710	6.50
14 500	3.42	4873	7.51	14 175	3.70	2879	8.10	661	6.36
15 329	3.09	3934	7.76	15 039	3.34	2413	8.07	617	6.22
15 967	2.83	3222	7.88	15 721	3.06	2051	8.00	579	6.09
16 525	2.61	2670	7.90	16 249	2.85	1767	7.88	544	5.97
16 956	2.43	2245	7.85	16 676	2.68	1543	7.74	513	5.85
		1916	7.76	17 069	2.53	1362	7.59	485	5.73

be caused by (1) underestimation of the *a priori* error, (2) leakage unaccounted for, and (3) an additional slower sorption process. The sorption isotherms of this work show identical qualitative behavior as data in the literature. The quantitative match is also good but the height of the sorption data and the linear decrease at high gas densities are 10% higher in this work than the data in the literature.

The high density part of the excess sorption isotherm can be interpreted with $m^{excess} = \bar{V}_{micropore}(\rho_{sorbed} - \rho)$, where $\bar{V}_{micropore}$ is the specific micropore volume of F400 and ρ_{sorbed} is the sorbed phase density. Humayun and Tomasko[11] discuss how $\bar{V}_{micropore}$ and ρ_{sorbed} are determined from excess sorption measurements. This concept is concisely repeated in Appendix G. Table IV shows the estimated sorbed phase densities and specific micropore volumes for all excess sorption isotherms.

The specific micropore volume of this work is the highest in Table IV. This is consistent with the excess sorption isotherm of this work (Fig. 2) being the highest. The differences in the specific micropore volumes of the F400 samples are expected to depend on the raw material and procedures used for F400 production. A 10% higher micropore volume is an acceptable variation in the properties of F400. The extrapolated sorbed phase density of this work falls between

the values reported by Tomasko and Gasem. All sorbed phase densities are in good agreement, with the value of Pini deviating the most. The cause of this deviation may be the limited accuracy of the regression (see Appendix G) due to the limited number of data points. The sorbed phase density is expected to be not susceptible to chemical and microporosity variations in the F400. The data are in agreement with this hypothesis (Table IV).

Figure 2 suggests that the measured excess isotherms of various authors agree within a constant proportionality factor. In agreement with this, we have found that the extrapolated sorbed phase density of CO_2 is more or less the same and the peak of the excess sorption is found at the same density value. This leads to the postulate that excess sorption is proportional to the specific micropore volume available for CO_2. Hence, the ratio between the various excess sorption isotherms is equal to the ratio of the specific micropore volumes for CO_2. This point of view is corroborated in Fig. 3,
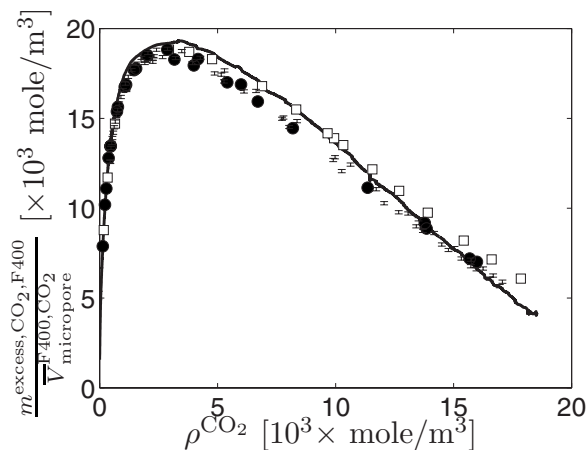
TABLE IV. Comparison data.

	T (K)	$\bar{V}_{micropore}^{F400,CO_2}$ [a] ($10^{-6} \times$ m^3/kg)	$\rho^{CO_2,F400}$ [a] ($10^3 \times$ mole/m^3)
Humayun and Tomasko[b]	318.1(5)	364	22.9(3)
Fitzgerald et al.[c]	318.1(5)	376	22.6(30)
Pini et al.[d]	318.4	393 ± 4	23.8 ± 0.1
This work[e]	318.11	429 ± 4	22.7 ± 0.2

[a]See the nomenclature in Table V.
[b]Reference 11.
[c]Reference 20.
[d]Reference 6.
[e]See Appendix G for details on regression.

FIG. 3. CO_2 excess sorption data on F400 at 318 K normalized by the specific micropore volume available. Plotted are this article (error bars), Gasem (filled circles), Tomasko (line), and Pini (open squares). All isotherms collapse on a single curve with most deviations within 1 mole/m^3 (5%).

which shows the CO_2 isotherms on F400 at 318 K normalized to their estimated specific micropore volumes, $m^{\text{excess}}/\bar{V}_{\text{micropore}}$.

IV. SUMMARY

The details of an improved manometric apparatus and its accompanying procedures for accurate measurements of supercritical CO_2 have been discussed. Two separate sets of experimental data of the excess sorption of CO_2 on Filtrasorb 400 at 318.11 K up to 17 069 mole/m³ have been presented. The variation between the two sets is 0.15 mole/kg at most, which agrees with the estimated *a priori* error of 0.06 mole/kg. The main source of uncertainty is in the determination of V^s through the He sorption experiment.

The isotherms of CO_2 on Filtrasorb 400 at 318 K from this work and the literature show similar behavior. The measurements in this work were 10% higher than the literature data. It was shown that the ratio between excess sorption isotherms was constant. This is consistent with an interpretation in terms of different specific micropore volumes. The good repeatability and excellent agreement with literature data confirm the accuracy of the improved manometric apparatus. Nomenclature is shown in Table V.

TABLE V. Nomenclature.

Symbol	Unit	Physical quantity
m^{excess}	mole/kg	(Gibbs) Excess sorption
m^{absolute}	mole/kg	Absolute sorption of gas
n^l	mole	Amount of leaked gas
n^{start}	mole	Amount in sample before experiment
V_i^r	m³	Reference cell volume used in step i
V^s	m³	Volume accessible to gas in the sample
$\bar{V}_{\text{micropore}}$	m³/kg	Specific micropore volume of sorbent
k	m³/s	Leak-rate coefficient
t	s	Time
ρ	mole/m³	Molar gas density
ρ_{sorbed}	mole/m³	Molar density of sorbed gas
ρ^*	kg/m³	Mass density
T	K	Temperature

		Superscripts
e		Equilibrium phase parameter
f		Filling phase parameter
Vacuum		Parameter at vacuum conditions at the start of the experiment
CO_2		Parameter is determined with or specific for CO_2
He		Parameter is determined with or specific for He
F400		Parameter is determined for F400

		Subscripts
i		Parameter for step i
N		Parameter for step N

APPENDIX A: DERIVATION OF DATA INTERPRETATION EQUATION

This appendix derives Eq. (1). It is a cumulative version (see also Ref. 34) of the equation presented in, e.g., Ref. 16 that uses a stepwise approach. Additional terms have been included to calculate leakage effects. The amount of excess sorbed gas is the difference between the amount of total and free gas in the sample cell, i.e.,

$$Mm_N^{\text{excess}} = n_N^{\text{total}} - V^s \rho_N^e. \tag{A1}$$

n_N^{total} is the total amount of gas in the sample cell. The amount of free gas in the sample cell is given by the volume accessible to gas and the density of the gas ($V^s \rho_N^e$).

The total amount of gas in the sample cell is given by

$$n_N^{\text{total}} = n^{\text{start}} + n_N^{\text{added}} - n_N^l, \tag{A2}$$

where n^{start} is the amount of gas at the start of the experiment, n_N^{added} is the summed amount of gas added via the reference cell, and n_N^l is the amount of gas leaked. The amount of leaked gas is given by Eq. (2) and derived from Appendix C. The amount of gas added (and extracted) via the reference cell is expressed by

$$n_N^{\text{added}} = \sum_{i=1}^N V_i^r (\rho_i^f - \rho_i^e). \tag{A3}$$

Using the initial condition of negligible gas at the start of the experiment, i.e., $n^{\text{start}} = 0$ and substituting Eqs. (A3) and (A2) in Eq. (A1), results in

$$m_N^{\text{excess}} = \sum_{i=1}^N \frac{V_i^r}{M}(\rho_i^f - \rho_i^e) - \frac{V^s}{M}\rho_N^e - \frac{n_N^l}{M}. \tag{A4}$$

APPENDIX B: INFLUENCE OF CONTAMINATION ON THE CARBON DIOXIDE SORPTION EXPERIMENT

Impurities in the CO_2 influence the accuracy of the excess sorption experiment. This is clear since the derivation of Eq. (1) only considers the presence of a single pure gas. The presence of impurities invalidates the EOS and the single component molar balance. Some He may remain in the sample cell because He is used during transport, for leak-rate determination, and for determination of the volume accessible to gas in the sample cell before the actual sorption experiment. Indeed, 15–25 kPa of He pressure remains in the sample cell after evacuation. This remnant He is the main impurity in the sorption experiments, i.e., impurities in the bottled CO_2 and contamination by air are negligible. Consideration of the He contamination and ignoring the effect of leakage modify Eq. (1) to

$$m_N^{\text{excess},CO_2,F400} = \sum_{i=1}^{N} \frac{V_i^r}{M}(\rho_i^{f,CO_2} - x_i^{e,CO_2}\rho_i^{e,He-CO_2})$$
$$- \frac{V^{s,He}}{M}x_N^{e,CO_2}\rho_N^{e,He-CO_2}, \qquad (B1)$$

where $\rho_i^{e,He-CO_2}$ is the density of the He–CO_2 mixture in step i. The CO_2 in the reference cells during the filling phase is considered to be pure. The mole fraction of carbon dioxide in the equilibrium phase x^{e,CO_2} can be obtained from

$$1 - x^{e,CO_2} = x^{e,He} = \frac{n^{He}/V^{s,He}}{(n^{He} + n^{CO_2})/V^{s,He}} = \frac{\rho^{He,vacuum}}{\rho^{e,He-CO_2}}. \quad (B2)$$

The density of the remnant He after evacuation $\rho^{He,vacuum}$ is constant throughout an experiment because V^s and n^{He} are constant and He sorption is small. It is assumed that the molar density of the mixture $\rho^{e,He-CO_2}$ can be approximated as an ideal mixture

$$\rho^{He-CO_2} = x^{CO_2}\rho^{CO_2} + (1 - x^{CO_2})\rho^{He}. \qquad (B3)$$

Using Eq. (B3) for the equilibrium phase into Eq. (B2) leads to a quadratic equation in x^{e,CO_2}. The solution of this equation is

$$x^{e,CO_2} = \frac{\rho^{e,He} - \frac{1}{2}(\rho^{e,CO_2} + E)}{\rho^{e,He} - \rho^{e,CO_2}}, \qquad (B4)$$

with $E = [4\rho^{vacuum,He}(\rho^{e,He} - \rho^{e,CO_2}) + (\rho^{e,CO_2})^2]^{1/2}$.

Now, the errors associated with the He contamination can be calculated. The remnant He pressures were 13 and 10 kPa for the two experiments. The following calculations are based on a remnant He pressure of 15 kPa and a constant temperature of 318.11 K. This corresponds to a He density after evacuation $\rho^{He,vacuum}$ of 5.7 mole/m^3. This number of moles of He is less than the total amount of CO_2 for any step i. The amount of He is 0.16% in the first step and decreases for additional steps. The remnant helium is thus negligible in comparison to the overall molar balance, i.e., the assumption of $n^{start}=0$ is justified. The value of 5.7 mole/m^3 for $\rho^{He,vacuum}$ corresponds to a CO_2 mole fraction values of 0.987 in the first measurement step and and drecreases for additional steps. The corresponding densities of He–CO_2 mixture are at most 0.13% less dense than pure CO_2.

Calculating mole fractions with Eq. (B4) and the corresponding mixture densities with Eq. (B3) and substitution in Eq. (B1) results in excess sorption values of 0.01–0.05 mole/kg higher than the values calculated without consideration of He contamination with Eq. (1) values. This systematic error is approximately as large as the other *a priori* errors (see Appendix E). Thus the experimental accuracy of this setup is limited at 0.01 to 0.05 mole/kg. Further improvements in accuracy require a decrease in the remnant pressure after evacuation. This constitutes the use of other valves in the setup.

APPENDIX C: LEAK-RATE MODEL

Leakage always occurs during manometric measurements and can be the main cause of inaccuracy. The ideal situation is that the leakage is negligible in comparison to the sorption. However, it was found that in sorption experiments

at pressures above 10 MPa and lasting several days leakage is often significant. Therefore, a leak-rate model is incorporated to correct for the leakage or to ensure that the effect of leakage is negligible. This model is only applicable for experiments with relatively small leakage. Appendix D discusses the conditions in which the model is applicable.

Combination of the mass balance equation ($V\partial_t\rho + R = 0$) with density driven mass transfer ($R = k\rho$) leads to

$$\rho^{leak}(t) = \rho^{exam}e^{-k(t-t^{exam})/V} \quad \text{for } t \geq 0, \qquad (C1)$$

where $\rho^{leak}(t)$ is the density of gas decreasing due to diffusion out of the cell of volume V. The used boundary condition is $\rho(t=t^{exam}) = \rho^{exam}$. k is the leak-rate constant. Atmospheric CO_2 concentration and air diffusion into the cell are disregarded. The amount of leaked gas for $0 \leq t \leq t^{exam}$ is then given by

$$n^{leak,I}(t) = V\rho^{exam}[e^{kt^{exam}/V} - e^{-k(t-t^{exam})/V}], \qquad (C2)$$

and for $t \geq t^{exam}$ by

$$n^{leak,II}(t) = V\rho^{exam}[1 - e^{-k(t-t^{exam})/V}] + n^{leak,I}(t^{exam}). \qquad (C3)$$

Equation (2) is Eq. (C3) with Eq. (C2) with parameters relevant for the apparatus. Leakage from the reference cell to the outside during the filling phase has no influence on the sorption measurements. The experiment specific leak-rate constants are determined with a He leak test before the sorption experiment. The CO_2 leak-rate constant is calculated with $k^{He}/k^{CO_2} \approx 3$. This dependency was observed in reference experiments with an empty setup. The CO_2 leak-rate constant is considered to be accurate within 20%.

APPENDIX D: DEMONSTRATION OF THE NEGLIGIBILITY OF THE INFLUENCE OF SORPTION ON THE LEAKAGE CORRECTION

The purpose of this appendix is to show that the leakage correction in Appendix C is useful as long as the characteristic times for sorption and leakage are sufficiently separated. For this reason, the influence of sorption on the leakage is investigated. We compare the case without the effect of sorption to the case with the effect of sorption to demonstrate that the effect is small.

Consider a vessel with a sorbent of mass M, a volume accessible to gas V, gas density $\rho^{forward}$, and sorption $m^{forward}$. The total number of moles in the vessel is $n^{total,forward} = V\rho^{forward} + Mm^{forward}$. The volume of the sorbed phase is considered negligible. Gas density and sorption are in equilibrium when $m^{forward} = \gamma\rho^{forward}$. Time dependent behavior of the density due to leakage is described with the same model as in Appendix C4: $V\frac{d\rho}{dt} = -k\rho$. Time dependent behavior of density and sorption is described by $M\frac{dm^{forward}}{dt} = \omega(\gamma\rho^{forward} - m^{forward})$. This is in line with the suggestion by Prigogine *et al.*[35] for the description of reaction rates near equilibrium. Combination results in

$$V\frac{d\rho^{forward}}{dt} + M\frac{dm^{forward}}{dt} = -k\rho^{forward}. \qquad (D1)$$

TABLE VI. Input parameters for the comparison of the forward and leak-rate models.

V (m^3)	M (kg)	ρ^0 $(mole/m^3)$	ρ^p $(mole/m^3)$
70×10^{-6}	35×10^{-3}	17×10^3	16×10^3

Using boundary conditions $\rho^{forward}(t=0)=\rho^0$ and $m^{forward}(t=0)=\omega\rho^p$, Eq. (D1) is solved by Laplace transforms. The time dependent density and amount of leaked gas of the forward model are given by

$$\rho^{forward}(t) = A(s^1 e^{s^1 t} - s^2 e^{s^2 t}) + B\left(\frac{e^{s^1 t}}{s^1} - \frac{e^{s^2 t}}{s^2}\right), \qquad (D2)$$

$$n^{forward}(t) = k[A e^{s^1 t} - A e^{s^2 t} + BC(t)], \qquad (D3)$$

with

$$A = \frac{\rho^0}{s^1 - s^2}, \quad B = \frac{\omega[M\gamma\rho^p + \rho^0 V]}{MV(s^1 - s^2)},$$

$$C(t) = \frac{e^{s^1 t} - 1}{s^1} - \frac{e^{s^2 t} - 1}{s^2},$$

$$s^{1,2} = \frac{-\frac{1}{2}kM - \frac{1}{2}M\gamma\omega - \frac{1}{2}V\omega \pm D}{MV},$$

and

$$D = \frac{1}{2}\sqrt{(kM + M\gamma\omega + V\omega)^2 - 4MVk\omega}.$$

Now the amount of leaked gas from the forward model with sorption can be compared to the amount of leaked gas from Appendix C without sorption. The ratio of these two leaked amounts $n^{leak,I}(\tau)/n^{forward}(\tau)$ is examined as a function of the characteristic sorption time, $\tau = \omega t/M$. Four values of γ, spanning realistic sorption magnitudes, were used. Other parameters are given in Table VI. Figure 4 shows that ignoring sorption leads to large errors when the characteristic time of sorption and leakage are similar ($\omega V/Mk=1$). Figure 5
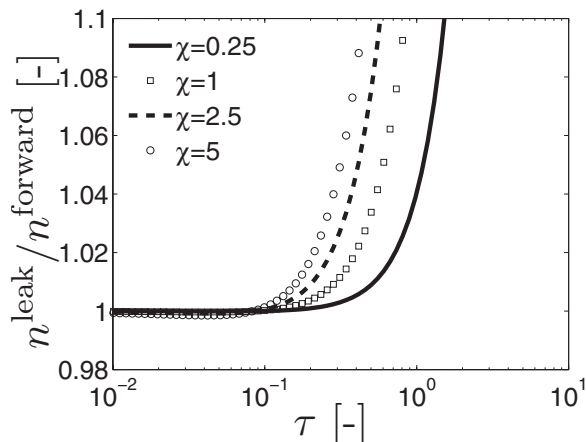

FIG. 4. Ratios of the leaked gas as calculated by the simple leak model and (D3) for $k_a V_f/Mk_l=1$ vs the characteristic sorption time. It is clear that the two models differ significantly for all values of χ and that the leak-rate model [Appendix C] is unusable.
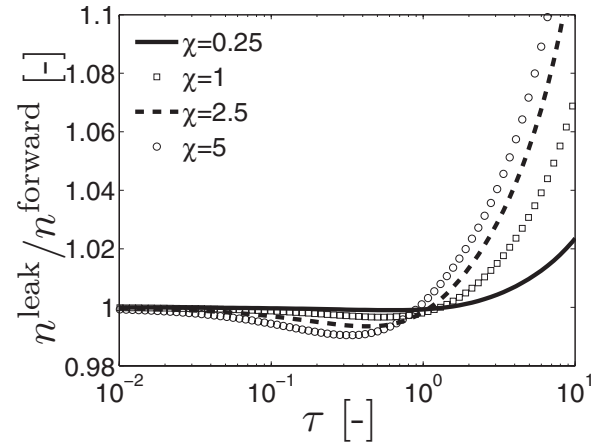

FIG. 5. Ratios of the leaked gas as calculated by the simple leak model and (D3) for $k_a V_f/Mk_l=25$ vs the characteristic sorption time. Deviation between the two models is 10% or less at $\tau \to 10$ for all values of χ. The leak-rate model [Appendix C] is applicable under these conditions.

shows that ignoring sorption leads to errors less than 10% for $\omega V/Mk=25$. This agrees with the simple notion that the amount of leakage is not influenced by sorption if sorption is much faster than leakage.

In our experiments $\omega V^s/Mk^{CO_2} \gg 25$, so the simple leak-rate model can be used to correct for the leakage. In experiments with $\frac{k_a V_f}{Mk_l} \le 25$, the simple leak-rate model may still be useful depending on the actual parameter values, especially γ. In such circumstances, a better approximation of the sorption isotherm will be required in order to prove the negligibility of sorption on the leakage correction. In this appendix a linear sorption isotherm is used because it allows an analytical expression for the relevant characteristic times.

APPENDIX E: *A PRIORI* UNCERTAINTY ANALYSIS

A useful tool to determine the accuracy of experimental data is an *a priori* analysis of the uncertainties associated with the experiment. An *a priori* uncertainty analysis supposes that the main uncertainty in the determination is the uncertainty in parameters used for the determination and calculates the error in the determined parameter as propagated by the parameter errors. In this article, the existence of other uncertainties has been safeguarded by rigorous specification of procedures and empty cell calibration experiments. The *a priori* error, calculated in this appendix, is estimated at 0.02–0.06 mole/kg. The error due to the presence of He is estimated at similar values. The observed discrepancy between the duplicate experiments has a maximum of 0.12 mole/kg. The discrepancy between the *a priori* uncertainty estimate and the maximum observed uncertainty is a factor of two. This is acceptable, but possible causes for the discrepancy are (1) underestimation of the *a priori* error, (2) unaccounted leakage, and (3) an additional slower sorption process.

It is important to emphasize the cumulative nature of manometric measurements. We use the term cumulative to stress that measurement O depends on all previous $(O-1)$ measurements. This means that (a) measured points are not independent within a data set, (b) an error in a data point
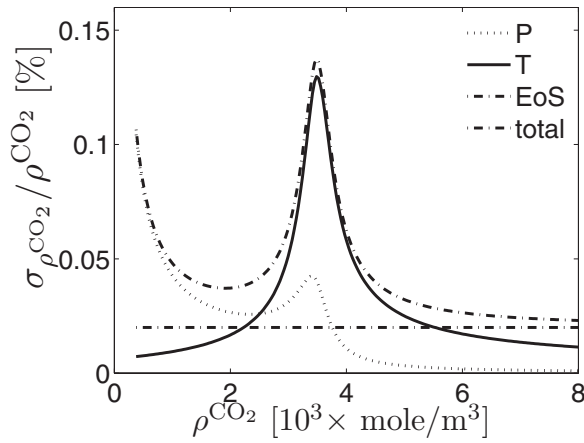
FIG. 6. Relative error in the density of CO_2 at 318.1 K for 1 kPa, 20 mK, and 0.2% in the EOS uncertainty (Ref. 36). Pressure uncertainty dominates at low densities since $\lim_{P \to 0} \delta P/P = \infty$. Temperature error dominates near $3.0 \times 10^3 \times$ mole/m³ where the density is very sensitive to temperature. The EOS error dominates at densities above $6.0 \times 10^3 \times$ mole/m³ where uncertainty in pressure and temperature is negligible.

FIG. 7. Uncertainty in the first sorption data set for the uncertainties in V^s, leakage, and ρ. The uncertainty in V^s is linear with density and dominates above $10.0 \times 10^3 \times$ mole/m³. The uncertainties in leakage and ρ are cumulative throughout the experiment and are high in the data. Uncertainty in the leakage is the main uncertainty in the desorption data below $7.0 \times 10^3 \times$ mole/m³.

propagates to all subsequent data points, and (c) the effect of leakage is cumulative throughout the experiment.

The uncertainties in the two reference cell volumes are 4 mm³ (0.1%) and 9 mm³ (0.07%). The uncertainty in the sample mass M is 0.03 g (0.09%) at most. The uncertainties in the reference cells and sample mass are a negligible effect in the sorption data. The uncertainties in the volume accessible to gas V^s, the leak-rate constant k, and the calculated densities ρ are significant and specifically considered in the following paragraphs.

The uncertainty in the gas accessible sample cell volume V^s is 0.1×10^{-6} m³ (0.2%) (see Appendix F). The uncertainty in excess sorption due to the uncertainty in V^s is given by

$$\delta_{V^s} m_N^{\text{excess}} = \frac{1}{2} |m_N^{\text{excess}}(V^s + \delta V^s; \dots)$$
$$- m_N^{\text{excess}}(V^s - \delta V^s; \dots)|. \quad \text{(E1)}$$

The uncertainty in the calculated leaked amounts is determined by the 20% uncertainty in the leak-rate constant k. The leak-rate model and its uncertainty are discussed in Appendix C. The uncertainty in the excess sorption due to the uncertainty in K is given by

$$\delta_l m_N^{\text{excess}} = \frac{1}{2} |m_N^{\text{excess}}(k - \delta k; \dots) - m_N^{\text{excess}}(k + \delta k; \dots)|. \quad \text{(E2)}$$

Uncertainties in the computed density values are caused by uncertainties in pressure, temperature, and the uncertainty of the used EOS. Figure 6 shows the uncertainty in ρ as calculated for these three uncertainties. The uncertainty in the excess sorption due to the uncertainties in the densities is calculated with

$$\delta_\rho m_N^{\text{excess}} = \frac{1}{M} \sqrt{\sum_{i=1}^{N} \{(V_i^r \delta \rho_i^f)^2 + [(V_i^r + \delta_{iN} V^s) \delta \rho_i^e]^2\}}. \quad \text{(E3)}$$
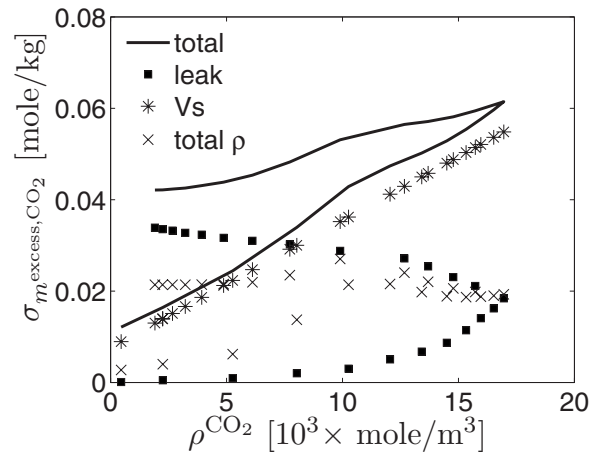
The *a priori* errors estimated with Eqs. (E1)–(E3) for the first sorption data set are shown in Fig. 7. The order of magnitude is similar for all three types of uncertainty. Total *a priori* uncertainty is thus between 0.02 and 0.06 mole/kg. The leaked amount and its error are negligible in the second shorter experiment. However, the *a priori* uncertainty estimate has not appreciably changed.

APPENDIX F: INTERPRETATION OF HE SORPTION EXPERIMENT

The volume accessible to gas in the sample cell V^s is an important parameter in the interpretation of sorption experiments. Previous work generally assumes that He sorption is negligible. However, both Sircar[37] and Gumma and Talu[38] demonstrated that this assumption is not always valid and suggested alternative experimental procedures to determine V^s. These procedures determine He sorption from its temperature dependency over a wide range of temperatures. These procedures were not adopted because of the limited operating temperature of the equipment. To incorporate the effect of He sorption on the Filtrasorb 400, an alternative approach is used based on the ansatz that He sorption on Filtrasorb 400 can be described with the Langmuir equation using Langmuir parameters b^{He} and s_∞^{He}. The Langmuir equation adequately describes the sorption of He on silicilates, as demonstrated by the data of Gumma and Talu.[38]

Using the Langmuir equation for m^{excess} in Eq. (A4) with remnant He (n^{start}) and neglecting leakage results in

$$\frac{M s_\infty^{\text{He}} b^{\text{He}} \rho_N^{e,\text{He}}}{1 + b^{\text{He}} \rho_N^{e,\text{He}}} = n^{\text{start,He}} + \sum_{i=1}^{N} V_i^r [\rho_i^{f,\text{He}} - \rho_i^{e,\text{He}}] - V^s \rho_N^{e,\text{He}}, \quad \text{(F1)}$$

with the remnant He (free and sorbed) given by

$$n^{\text{start,He}} = \rho^{\text{He,vacuum}} V^s + \frac{M s_\infty^{\text{He}} b^{\text{He}} \rho^{\text{He,vacuum}}}{1 + b^{\text{He}} \rho^{\text{He,vacuum}}}. \quad \text{(F2)}$$
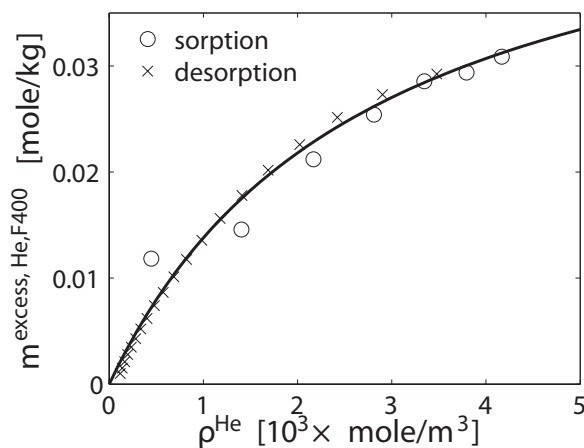
FIG. 8. The fitted He Langmuir isotherm (line) is consistent with the sorption (○) and desorption (x) measurements. The fitted values of the Langmuir equation are $s_\infty^{He} = 0.05 \pm 0.03$ mole/kg and $b^{He} = 0.4 \pm 0.2 \times 10^{-3}$ m^3/mole.

Nomenclature is given in Table V. The parameters V^s, b^{He}, and s_∞^{He} are determined by fitting Eq. (F1) to the He density values calculated from the measured pressures and temperatures.[39] The "lsqnonlin" function from the Optimization Toolbox™ in MATLAB® (Ref. 40) is used for fitting.

Figure 8 confirms the ansatz that a Langmuir equation can describe He sorption on Filtrasorb 400. Consideration of the He sorption decreases the V^s value by 2% and the uncertainty in its determination by a factor of four.

APPENDIX G: SPECIFIC MICROPORE VOLUME AND SORBED PHASE DENSITY DETERMINATION FROM THE EXCESS SORPTION ISOTHERM

The absolute sorbed amount is by definition

$$m^{absolute} \equiv \rho_{sorbed} \bar{V}_{micropore},$$

where $\bar{V}_{micropore}$ is the specific micropore volume filled with sorbed gas and ρ_{sorbed} is the density of the sorbed gas. The relationship between the excess sorption, m^{excess}, and the absolute sorption is

$$m^{excess} = m^{absolute} - \rho \bar{V}_{micropore} = (\rho_{sorbed} - \rho) \bar{V}_{micropore}, \tag{G1}$$

with ρ as the gas density. Eq. (G1) shows that excess sorption is zero when the sorbed phase density equals the gas phase density ($\rho_{sorbed} = \rho$ at $m^{excess} = 0$). It is assumed that both the filled specific micropore volume and density of the sorbed phase are approximately constant at high gas densities, i.e., in the linear part of the excess sorption isotherm in Fig. 2. It follows that m^{excess} is a linear function of ρ with $-\bar{V}$

TABLE VII. Accuracy of the linear regressions to estimate specific micropore volume and sorbed phase density.

	T (K)	R^2 (−)	$\sigma_{m^{excess}}$ (mole/kg)
Pini[a]	318.4	0.9992	0.04
This work[b]	318.11	0.997	0.1

[a]Parameters regressed from data with $\rho^{CO_2} > 6.0 \times 10^3$ mole/m^3 (Ref. 6).
[b]Parameters regressed from sorption data with $\rho^{CO_2} > 4.0 \times 10^3$ mole/m^3.

as the slope. Thus both the density of the sorbed phase and the specific micropore volume can be determined from a linear regression through the high density excess sorption data .

Table VII shows the quality of the linear regressions. The standard deviation from linear regression $\sigma_{m^{excess}}$ is in good agreement with the repeatability and *a priori* error (see Sec. III and Appendix E). Calculations show that the error of our measurements is not normally distributed, which is expected from the *a priori* analysis.

[1]C. M. White, D. H. Smith, K. L. Jones, A. L. Goodman, S. A. Jikich, R. B. LaCount, S. B. DuBose, E. Ozdemir, B. I. Morsi, and K. T. Schroeder, Energy Fuels **19**, 659 (2005).
[2]R. Pini, S. Ottiger, A. Rajendran, G. Storti, and M. Mazzotti, Adsorption **14**, 133 (2008).
[3]R. Sakurovs, S. Day, S. Weir, and G. Duffy, Energy Fuels **21**, 992 (2007).
[4]A. L. Goodman, A. Busch, R. M. Bustin, L. Chikatamarla, S. Day, G. J. Duffy, J. E. Fitzgerald, K. A. M. Gasern, Y. Gensterblum, C. Hartman, C. Jing, B. M. Krooss, S. Mohammed, T. Pratt, R. L. Robinson, V. Romanov, R. Sakurovs, K. Schroeder, and C. M. White, Int. J. Coal Geol. **72**, 153 (2007).
[5]J. S. Bae and S. K. Bhatia, Energy Fuels **20**, 2599 (2006).
[6]R. Pini, S. Ottiger, A. Rajendran, G. Storti, and M. Mazzotti, Adsorption **12**, 393 (2006).
[7]S. Ottiger, R. Pini, G. Storti, M. Mazzotti, R. Bencini, F. Quattrocchi, G. Sardu, and G. Derui, Environ. Prog. **25**, 355 (2006).
[8]R. Staudt, A. Herbst, S. Beutekamp, and P. Harting, Adsorption **11**, 379 (2005).
[9]W. H. Gao, D. Butler, and D. L. Tomasko, Langmuir **20**, 8083 (2004).
[10]T. Hocker, A. Rajendran, and M. Mazzotti, Langmuir **19**, 1254 (2003).
[11]R. Humayun and D. L. Tomasko, AIChE J. **46**, 2065 (2000).
[12]T. Hoshino, K. Nakamura, and Y. Suzuki, Biosci., Biotechnol., Biochem. **57**, 1670 (1993).
[13]W. M. Jones, P. J. Isaac, and D. Phillips, Trans. Faraday Soc. **55**, 1953 (1959).
[14]A. Busch, Y. Gensterblum, and B. M. Krooss, Energy Fuels **21**, 1640 (2007).
[15]A. Busch, Y. Gensterblum, B. M. Krooss, and N. Siemons, Int. J. Coal Geol. **66**, 53 (2006).
[16]N. Siemons and A. Busch, Int. J. Coal Geol. **69**, 229 (2007).
[17]L. Zhou, S. P. Bai, W. Su, J. Yang, and Y. P. Zhou, Langmuir **19**, 2683 (2003).
[18]B. M. Krooss, F. van Bergen, Y. Gensterblum, N. Siemons, H. J. M. Pagnier, and P. David, Int. J. Coal Geol. **51**, 69 (2002).
[19]J. H. Chen, D. S. H. Wong, C. S. Tan, R. Subramanian, C. T. Lira, and M. Orth, Ind. Eng. Chem. Res. **36**, 2808 (1997).
[20]J. E. Fitzgerald, Z. Pan, M. Sudibandriyo, R. L. Robinson, K. A. M. Gasem, and S. Reeves, Fuel **84**, 2351 (2005).
[21]M. Sudibandriyo, Z. J. Pan, J. E. Fitzgerald, R. L. Robinson, and E. A. M. Gasem, Langmuir **19**, 5323 (2003).
[22]P. Pendleton and A. Badalyan, Adsorption **11**, 61 (2005).
[23]E. Robens, J. U. Keller, C. H. Massen, and R. Staudt, J. Therm Anal. Calorim. **55**, 383 (1999).
[24]F. Rouquerol, J. Rouquerol, and K. Sing, *Adsorption by Powders and Porous Solids*, 1st ed. (Academic, New York, 1999).
[25]W. S. Borghard, E. W. Sheppard, and H. J. Schoennagel, Rev. Sci. Instrum. **62**, 2801 (1991).
[26]M. H. Kim, C. J. Glinka, and R. N. Carter, Rev. Sci. Instrum. **76**, 10 (2005).
[27]S. D. Hersee and J. M. Ballingall, J. Vac. Sci. Technol. A **8**, 800 (1990).
[28]D. P. Broom, Int. J. Hydrogen Energy **32**, 4871 (2007).
[29]J. M. Blackman, J. W. Patrick, and C. E. Snape, Carbon **44**, 918 (2006).
[30]E. Poirier, R. Chahine, A. Tessier, and T. K. Bose, Rev. Sci. Instrum. **76**, 055101 (2005).
[31]M. Mavor, C. Hartman, and T. Pratt, Proceedings of International Coalbed Methane Symposium, University of Alabama, Tuscaloosa, 2004 (unpublished).
[32]R. C. Reid, J. M. Prausnitz, and B. E. Poling, *The Properties of Gases and Liquids* (McGraw-Hill, New York, 1987).
[33]R. Span and W. Wagner, J. Phys. Chem. Ref. Data **25**, 1509 (1996).
[34]P. van Hemert, K.-H. A. A. Wolf, and J. G. Maas, Proceedings of International Coalbed Methane Symposium, University of Alabama, Tuscaloosa,

2006.

[35] I. Prigogine, P. Outer, and C. L. Herbo, J. Phys. Colloid Chem. **52**, 321 (1948).

[36] J. Klimeck, R. Kleinrahm, and W. Wagner, J. Chem. Thermodyn. **33**, 251 (2001).

[37] S. Sircar, AIChE J. **47**, 1169 (2001).

[38] S. Gumma and O. Talu, Adsorption **9**, 17 (2003).

[39] M. R.D. and A. V.D., Proceedings of Advances in Cryogenic Engineering, 1990, p. 1465.

[40] http://www.mathworks.com/, 2008.